Atmos. Chem. Phys., 24, 4017–4027, 2024
https://doi.org/10.5194/acp-24-4017-2024

Atmospheric Chemistry and Physics
Open Access
EGU

Research article

A large role of missing volatile organic compound reactivity from anthropogenic emissions in ozone pollution regulation

Wenjie Wang[1,2], Bin Yuan[1], Hang Su[2], Yafang Cheng[2], Jipeng Qi[1], Sihang Wang[1], Wei Song[3], Xinming Wang[3], Chaoyang Xue[2], Chaoqun Ma[2], Fengxia Bao[2], Hongli Wang[4], Shengrong Lou[4], and Min Shao[1]

[1]Institute for Environmental and Climate Research, Jinan University, Guangzhou 511443, China
[2]Multiphase Chemistry Department, Max Planck Institute for Chemistry, 55128 Mainz, Germany
[3]State Key Laboratory of Organic Geochemistry, Guangzhou Institute of Geochemistry, Chinese Academy of Sciences, Guangzhou 510640, China
[4]State Environmental Protection Key Laboratory of Formation and Prevention of Urban Air Pollution Complex, Shanghai Academy of Environmental Sciences, Shanghai 200233, China

Correspondence: Wenjie Wang (wenjie.wang@mpic.de) and Bin Yuan (byuan@jnu.edu.cn)

Received: 8 November 2023 – Discussion started: 15 December 2023
Revised: 14 February 2024 – Accepted: 20 February 2024 – Published: 4 April 2024

Abstract. There are thousands of volatile organic compound (VOC) species in ambient air, while existing techniques can only detect a small part of them (approximately several hundred). The large number of unmeasured VOCs prevents us from understanding the photochemistry of ozone and aerosols in the atmosphere. The major sources and photochemical effects of these unmeasured VOCs in urban areas remain unclear. The missing VOC reactivity, which is defined as the total OH reactivity of the unmeasured VOCs, is a good indicator for constraining the photochemical effect of unmeasured VOCs. Here, we identified the dominant role of anthropogenic emission sources in the missing VOC reactivity (accounting for up to 70 %) by measuring missing VOC reactivity and tracer-based source analysis in a typical megacity in China. Omitting the missing VOC reactivity from anthropogenic emissions in model simulations will remarkably affect the diagnosis of sensitivity regimes for ozone formation, overestimating the degree of VOC-limited regimes by up to 46 %. Therefore, a thorough quantification of missing VOC reactivity from various anthropogenic emission sources is urgently needed for constraints of air quality models and the development of effective ozone control strategies.

1 Introduction

Volatile organic compounds (VOCs) are key precursors of major photochemical pollutants, including ozone (O_3) and secondary organic aerosols (Atkinson, 2000; Atkinson and Arey, 2003). Severe O_3 and particle pollution is frequently related to high emissions of VOCs (Atkinson and Arey, 2003; Monks et al., 2015). There exist thousands of VOC species in ambient air that are emitted from either natural processes or anthropogenic activities (Goldstein and Galbally, 2007). No one instrument can capture all VOCs out there, and even when they can be measured, there is information missing on identification and properties (Yuan et al., 2017; Wang et al., 2014). A gas chromatograph–mass spectrometer/flame ionization detector (GC–MS/FID) can measure C_2–C_{12} non-methane hydrocarbons (NMHCs) and C_2–C_6 oxygenated VOCs (OVOCs) but cannot measure NMHCs and OVOCs with larger carbon numbers (Wang et al., 2014). A proton-transfer-reaction time-of-flight mass spectrometer (PTR-ToF-MS) is able to measure a huge number of OVOCs, aromatics and several alkanes but cannot measure most alkanes and alkenes and cannot distinguish isomers (Yuan et al., 2017). The 2,4-dinitrophenylhydrazine (DNPH) or high-performance liquid chromatography (HPLC) method

can measure several carbonyls but cannot measure non-polar organic species (Wang et al., 2009). The two-dimensional GC is able to measure some intermediate-volatile and semivolatile non-polar organics (Song et al., 2022). A lack of standard gases prevents these technologies from accurate quantification even if these technologies can identify more VOC species. In general, many branched alkenes, OVOCs with complex functional groups, intermediate-volatile and semivolatile organics and complex biogenic VOCs cannot currently be well quantified even if they can be identified by instruments. As a result, the total amount of VOCs in ambient air has generally been underestimated. Currently, emission inventories used in air quality models such as the Community Emissions Data System (CEDS) emission inventory and the Multi-resolution Emission Inventory for China (MEIC) only include the VOC species that can be measured, such as some C_1–C_9 hydrocarbons and simple-structure OVOCs with a small carbon number ($< C_6$). This will lead to an underestimation of the photochemical effect of the total VOCs and thus causes uncertainties in predicting secondary pollution. The quantification of the unmeasured VOCs is crucial for assessing secondary pollution precisely.

The total OH reactivity (R_{OH}), which can be directly measured, is an index for evaluating the amount of reductive pollutants in terms of ambient OH loss. The total OH reactivity is defined as

$$R_{OH} = \sum_i k_{OH+X_i}[X_i], \quad (1)$$

where X represents a reactive species including carbon monoxide (CO), nitrogen oxides (NO_X) and VOCs, and k_{OH+X_i} is the reaction rate constant for the oxidation of species X by OH. The measured R_{OH} is higher than that calculated based solely on the measured reactive species, and the difference between them is mostly from unmeasured VOCs (Yang et al., 2017). Missing VOC reactivity (missing VOC_R), defined as the VOC reactivity (VOC_R) of all unmeasured VOCs, can be obtained by subtracting the calculated R_{OH} from the measured R_{OH}:

$$\text{missing } VOC_R = \text{measured } R_{OH}\text{-calculated } R_{OH}, \quad (2)$$

$$\text{calculated } R_{OH} = \sum_i k_{OH+\text{reactive species}_i}[\text{reactive species}_i], \quad (3)$$

where "reactive species" represents measured VOCs and "reactive inorganic species" includes carbon monoxide (CO), nitric oxide (NO), nitrogen dioxide (NO_2), O_3, sulfur dioxide (SO_2), nitrous acid (HONO), and so on. The missing VOC_R provides a constraint for evaluating the photochemical roles of unmeasured VOCs in the atmosphere (Sadanaga et al., 2005; Yang et al., 2016b). The inclusion of the missing VOC_R can help to improve the performance of the box model and air quality models in simulating photochemistry processes. A relatively high missing VOC_R has been found in forests (Di Carlo et al., 2004; Hansen et al., 2014; Nakashima et al., 2014; Nölscher et al., 2016; Praplan et al., 2019), urban areas (Shirley et al., 2006; Yoshino et al., 2006; Dolgorouky et al., 2012; Yang et al., 2017), and suburban areas (Kovacs et al., 2003; Yang et al., 2017; Fuchs et al., 2017; Lou et al., 2010), accounting for 10 %–75 % of the total R_{OH}. Given that the total VOC_R is one part of the total R_{OH}, missing VOC_R would account for a larger percentage of the total VOC_R (> 10 %–75 %).

The potential sources of missing VOC_R include anthropogenic emissions, biogenic emissions, soil emissions, and photochemical production (Yang et al., 2016b). Previous studies have reported that the missing VOC_R in forest areas was mainly from direct emissions or photochemical oxidation of biogenic VOCs (Di Carlo et al., 2004; Hansen et al., 2014; Nakashima et al., 2014; Nölscher et al., 2016; Praplan et al., 2019). Nevertheless, the dominant source of the missing VOC_R in urban and suburban areas remains unclear or under debate.

Surface O_3 pollution has become a major public health concern in cities worldwide (Paoletti et al., 2014; Lefohn et al., 2018). A critical issue in determining an emission control strategy for ozone pollution is to understand the relative benefits of NO_x and VOC emission controls. This is generally framed in terms of ozone precursor sensitivity, i.e., whether ozone production is NO_X-limited or VOC-limited (Kleinman, 1994; Sillman et al., 1990). Nevertheless, the effect of missing VOCs on ozone precursor sensitivity has not been well understood yet. Given that the missing VOC_R could potentially account for a large part of the total VOC_R, clearly clarifying the role of missing VOC_R in determining ozone precursor sensitivity is an urgent need for the diagnosis of ozone sensitivity regimes and the formulation of an effective emission reduction roadmap.

China has become a global hotspot of ground-level ozone pollution in recent years (Lu et al., 2018; Wang et al., 2022). The Pearl River Delta (PRD) remains one of the most O_3-polluted regions in China (Li et al., 2022), although many control measures have been attempted. Here, we measured R_{OH} in Guangzhou, a megacity in the PRD, and quantified the missing VOC_R. The dominant source of the missing VOC_R and its impact on ozone precursor sensitivity were comprehensively investigated.

2 Method

2.1 Overview of the measurement

The field campaign was conducted from 25 September to 30 October 2018 continuously at an urban site in downtown Guangzhou (113.2° E, 23° N). The sampling site is located on the ninth floor of a building on the campus of the Guangzhou Institute of Geochemistry, Chinese Academy of Sciences, 25 m above ground level. This site is primarily influenced by industrial and vehicular emissions. ROH, VOCs, NO_X, O_3, HONO, SO_2, CO, photolysis frequencies, and meteorological factors were simultaneously measured during the measurement period.

2.2 R_{OH} measurement

The total R_{OH} was measured by the comparative reactivity method (CRM) (Sinha et al., 2008). The CRM system consists of three major components, i.e., an inlet and calibration system, a reactor, and a measuring system. Here, pyrrole (C_4H_5N) was used as the reference substance in the CRM, and its concentration was quantified by a quadrupole proton-transfer-reaction mass spectrometer (PTR-MS) (Ionicon Analytik GmbH, Innsbruck, Austria). The CRM system was calibrated by propane, propene, toluene standards, and 16 VOC mixed standards (acetaldehyde, methanol, ethanol, isoprene, acetone, acetonitrile, methyl vinyl ketone, methyl ethyl ketone, benzene, toluene, o-xylene, α-pinene, 1,2,4-trimethylbenzene, phenol, m-cresol, and naphthalene). Measured and calculated R_{OH} agreed well within 15 % for all the calibrations. The R_{OH} measurement by the CRM method is interfered by ambient nitric oxide (NO), which produces additional OH radicals via the reaction of HO_2 radicals with NO (Sinha et al., 2008). To correct this interference, a series of experiments were conducted by introducing different levels of NO (0–160 ppb) and given amounts of VOC into the CRM reactor. A correction curve was acquired from these NO interference experiments, which can be used to correct the R_{OH} thanks to the simultaneous measurement of ambient NO concentrations (Supplement S1; Fig. S1). The detection limits of the CRM method were around 2.5 s^{-1}, and the total uncertainty was estimated to be about 15 %. The CRM method has been successfully applied to measure OH reactivity in urban areas with high NO_X levels in previous studies (Dolgorouky et al., 2012; Yang et al., 2017; Hansen et al., 2015). The intercomparison between the CRM method and the pump–probe technique indicates that the CRM method can be used under high-NO_X conditions ($NO_X > 10$ ppb) if a NO_X-dependent correction is applied (Hansen et al., 2015).

2.3 VOC measurements

NMHCs were measured using a GC–MS/FID system coupled with a cryogen-free preconcentration device (Wang et al., 2014). The system contains two-channel sampling and GC column separation, which are able to measure C_2–C_5 hydrocarbons with the FID in one channel and measure C_5–C_{12} hydrocarbons using an MS detector in the other channel. After removal of water vapor, VOCs were trapped at −155° in a deactivated quartz capillary column (15 cm × 0.53 mm ID) and a porous-layer open tubular (PLOT) capillary column (15 cm × 0.53 mm ID) for the MS channel and the FID channel, respectively. The system was calibrated weekly by TO-15 (Air Environmental Inc., USA) and PAMS gas standards (Spectra Gases Inc., USA). Detection limits for various compounds were in the range of 0.002–0.070 ppbv. A total of 56 NMHC species were measured (Table S1). The time resolution of the measurement was 1 h. The uncertainties of VOC measurements by GC–MS/FID are in the range of 15 %–20 %. More details of this method can be found in previous studies (Wang et al., 2014; Yuan et al., 2012).

An online PTR-ToF-MS (Ionicon Analytic GmbH, Innsbruck, Austria) with H_3O^+ and NO^+ ion sources was also used to measure VOCs. During the campaign, the PTR-ToF-MS automatically switched between H_3O^+ and NO^+ chemistry every 10–20 min. The H_3O^+ mode was used to measure OVOCs and aromatics, while the NO^+ model was used to measure alkanes with more carbons (C_8–C_{20}). When running in the H_3O^+ ionization mode, the drift tube was at a temperature of 50°, a pressure of 3.8 mbar, and a voltage of 920 V, leading to an operating E/N (E is the electric field, and N is the number density of the gas in the drift tube) ratio of 120 Td. When running in the NO^+ ionization mode, the drift tube was at a temperature of 50°, a pressure of 3.8 mbar, and a voltage of 470 V, leading to an operating E/N ratio of 60 Td. The PTR-ToF-MS technique is capable of measuring OVOCs and higher alkanes that a GC–MS/FID cannot measure (Wu et al., 2020; C. Wang et al., 2020). The time resolution of PTR-ToF-MS measurements was 10 s. A total of 31 VOCs were calibrated using either gas or liquid standards (Table S2). For other measured VOCs, we used the method proposed by Sekimoto et al. (2017) to determine the relationship between VOC sensitivity and kinetic rate constants for proton-transfer reactions of H_3O^+ with VOCs. The fitted line was used to determine the concentrations of those uncalibrated species. The uncertainties of the concentrations for uncalibrated species were about 50 % (Sekimoto et al., 2017). With this method, PTR-ToF-MS can additionally measure 128 VOCs, which were included in the analysis of this study. The detailed information for this method can be found in Wu et al. (2020), and all VOC species measured by a PTR-ToF-MS were provided in Table S4 of that article. The PTR-ToF-MS is capable of measuring additional VOC species that GC–MS/FID cannot measure, including alkanes with more carbons (C_{12}–C_{20}) and OVOCs, including aldehydes, ketones, carboxylic acids, alcohols, and nitrophenols. Formaldehyde (HCHO) was measured by a custom-built instrument based on the Hantzsch reaction and absorption photometry (Xu et al., 2022).

2.4 Other measurements

Nitrous acid (HONO) was measured by a custom-built LOPAP (long-path-absorption photometer) based on wet chemical sampling and photometric detection (Yu et al., 2022). The uncertainty of the measurement was 8 %. NO_X, O_3, SO_2, and CO were measured by an NO_X analyzer (Thermo Scientific, Model 42i), an O_3 analyzer (Thermo Scientific, Model 49i), an SO_2 analyzer (Thermo Scientific, Model 43i), and a CO analyzer (Thermo Scientific, Model 48i), respectively. The meteorological data, including temperature (T), relative humidity (RH), and wind speed and direction (WS, WD), were recorded by Vantage Pro2 Weather Station (Davis Instruments Inc., Vantage Pro2) with

a time resolution of 1 min. Photolysis frequencies of O_3, NO_2, HONO, H_2O_2, HCHO, and NO_3 were measured by a spectrometer (Focused Photonics Inc., PFS-100) (Shetter and Müller, 1999; Wang et al., 2019).

2.5 Multiple linear regression

Multiple linear regression (MLR) has been successfully applied to quantify the sources of air pollutants (Li et al., 2019; Yang et al., 2016a). In this study, a tracer-based MLR analysis was used to decouple the individual contributions of anthropogenic emissions, secondary production, biogenic emissions, and background level to missing VOC_R, as shown in Eq. (4).

$$\text{Missing VOC}_\text{R} = a\Delta\text{CO} + b[\text{O}_X] + c[\text{isoprene}_\text{initial}] + C_\text{background} \quad (4)$$

O_X is defined as $O_3 + NO_2$. ΔCO, $[O_X]$, and $[\text{isoprene}_\text{initial}]$ are concentrations of tracers for anthropogenic emissions, secondary production, and biogenic emissions, respectively. ΔCO is the relative change between the ambient CO and background CO of 150 ppb (C. Wang et al., 2020). $[\text{isoprene}_\text{initial}]$ represents the initial concentration of isoprene from biogenic emissions that has not undergone any photochemical reactions, which is calculated from the observed isoprene and its photochemical products methyl vinyl ketone (MVK) and methacrolein (MACR) (Xie et al., 2008). $C_\text{background}$ indicates the background level of missing VOC_R. a, b, c, and $C_\text{backgound}$ are coefficients fitted by the multiple linear regression.

2.6 Observation-based box model

A zero-dimensional box model coupled with the Master Chemical Mechanism (MCM) v3.3.1 (Jenkin et al., 2003) was used to simulate the photochemical production of RO_X ($RO_X = OH + HO_2 + RO_2$) radicals and O_3 during the field campaign. The model was constrained by the observations of meteorological parameters, photolysis frequencies, VOCs, NO, NO_2, O_3, CO, SO_2, and HONO. The model runs were performed in a time-dependent mode with a time resolution of 1 h and a spin-up of 4 d. A 24 h lifetime was introduced for all simulated species, including secondary species and radicals, to approximately simulate dry deposition and other losses of these species (Lu et al., 2013; W. Wang et al., 2020). Sensitivity tests show that this assumed physical loss lifetime has a relatively small influence on RO_X radicals and ozone production rates.

Measured OVOCs such as HCHO, acetaldehyde, and acetone were constrained in the model, and unmeasured OVOCs were simulated according to the photochemical oxidation of NMHCs by OH radicals. RO_2, HO_2, and OH radicals were simulated by the box model to calculate the net O_3 production rate ($P(O_3)$) and O_3 loss rate ($L(O_3)$) as shown in Eqs. (5) and (6) as derived by Mihelcic et al. (2003).

$$P(\text{O}_3) = k_{\text{HO}_2+\text{NO}}[\text{HO}_2][\text{NO}] + \sum_i \left(k^i_{\text{RO}_2+\text{NO}}\left[\text{RO}^i_2\right][\text{NO}]\right) - k_{\text{OH}+\text{NO}_2}[\text{OH}][\text{NO}_2] - L(\text{O}_3) \quad (5)$$

$$L(\text{O}_3) = (\theta j\left(\text{O}^1D\right) + k_{\text{OH}+\text{O}_3}[\text{OH}] + k_{\text{HO}_2+\text{O}_3}[\text{HO}_2] + \sum_j \left(k^j_{\text{alkene}+\text{O}_3}\left[\text{alkene}^j\right]\right)[\text{O}_3] \quad (6)$$

θ is the fraction of O^1D from ozone photolysis that reacts with water vapor, and i and j represent the number of species of RO_2 and alkenes, respectively.

The box model was used to evaluate the impact of missing VOC_R on the O_3 production rate. In the base scenario, the box model was constrained by all measured inorganic and organic gases, but the missing VOC_R was not considered. To consider the missing VOC_R in the box model, we additionally increased the concentration of NMHCs to exactly compensate for the missing VOC_R by multiplying a factor on the basis of measured NMHC concentrations. We simulated four scenarios by increasing the concentration of (1) n-pentane, (2) ethylene, (3) toluene, and (4) all measured 56 NMHCs. For the scenario of increasing all 56 NMHCs, concentrations of the 56 NMHC species were increased by multiplying the same factor. Given that the VOC_R of unconstrained secondary products increases with the increase in the concentration of NMHCs, several attempts for different values are needed to determine the increasing factor.

3 Results and discussion

3.1 Quantification of missing VOC_R during the campaign

Figure 1 shows the time series of measured R_{OH}, calculated R_{OH} according to all measured reactive gases, and missing VOC_R (the gap between the measured and calculated R_{OH}) in Guangzhou. By using a GC-MS/FID, we measured 56 NMHCs. By using a PTR-ToF-MS, we measured 159 VOCs, and 128 of them were difficult to measure before. In addition to the alkanes with carbons less than 12, a PTR-ToF-MS can measure alkanes with more carbons (C_{12}–C_{20}). With regard to OVOCs, not only common OVOC species including formaldehyde and C_2–C_4 carbonyls, but also carbonyls with more carbons (C_5–C_{10}) and some N-containing OVOC species such as nitrophenol and methyl nitrophenol were measured by a PTR-ToF-MS. Thanks to these additional measured VOCs, the measured R_{OH} was close to the calculated R_{OH} within 20 % in most periods. In some periods the missing VOC_R was negative, which is probably due to the uncertainty in the measurements of R_{OH} and reactive gases. The negative missing VOC_R primarily occurred in the afternoon (12:00–17:00) when the photochemistry was most active. Nevertheless, there were still some days exhibiting

remarkable missing VOC_R. Days with a missing VOC_R of more than 25 % of the total R_{OH}, i.e., high missing-VOC_R days, are indicated by yellow background in Fig. 1a. The largest missing VOC_R occurred on 15, 16, 25, and 26 October, with average values of 16 s^{-1}. During the period of 24 to 26 October, the total R_{OH} was highest and the missing VOC_R was also relatively high among all the days. Figure 1b shows the contribution of different species classifications to the total R_{OH} during high missing-VOC_R days. Inorganic species, NMHCs, and OVOCs account for 34 %, 13 %, and 14 % of the total R_{OH}, respectively, with missing VOC_R accounting for 39 %. The fraction of missing VOC_R (39 %) during the high missing-VOC_R days is comparable to measurements in Los Angeles in 2010 (Griffith et al., 2016) and in Seoul in 2016 (Sanchez et al., 2021).

We evaluated the uncertainty of the missing VOC_R. The uncertainty of the R_{OH} measurement was 15 %. In addition, according to reports by the Jet Propulsion Laboratory (Burkholder et al., 2020), reaction rate constants used for the calculation of R_{OH} in Eq. (3) have uncertainties of 5 %–30 %, depending on different species. We took the uncertainties in the reaction rate constants and the measurements of all the reactive gases into account when calculating R_{OH}, according to error propagation. As a result, the uncertainties in the missing VOC_R are 3.8 and 5.2 s^{-1} for the whole measurement period and the high missing-VOC_R days, respectively. The average missing VOC_R during the high missing-VOC_R days is 13 s^{-1}, which is significantly higher than the uncertainty of 5.2 s^{-1}, suggesting that the missing VOC_R really exists during the high missing-VOC_R days.

3.2 The sources of missing VOC_R

To explore the sources of missing VOC_R during the whole measurement period, we investigated the correlation between missing VOC_R and tracers characterizing primary emissions (CO, NO_X, and NMHCs) and secondary production ($O_X \equiv O_3 + NO_2$ and formic acid). The correlation of missing VOC_R with CO, reactivity of NMHCs ($NMHC_R$), and NO_X is moderate, with a correlation coefficient (R) in the range of 0.47–0.56 (Figs. 2a and b, S2) while there is no significant correlation of missing VOC_R with O_X and formic acid (Figs. 2c and S2). Furthermore, there is no significant correlation between missing VOC_R and acetonitrile, which is a tracer of biomass burning (de Gouw et al., 2003; Wang et al., 2007) (Fig. S2), indicating that biomass burning was not a major contributor to missing VOC_R during this campaign. In terms of the diurnal variation, the missing VOC_R was higher in the morning (07:00–10:00) and evening (18:00–22:00), when the anthropogenic emissions, especially vehicle exhaust, were intensive, and was lower in the afternoon, when the photochemistry was most active (Fig. 2d). The diurnal profile of missing VOC_R was similar to those of CO, NO_X, and $NMHC_R$. In contrast, the diurnal profiles of secondary species, including O_X, formic acid, and acetic acid, which peaked in the afternoon, evidently differ from the diurnal profile of missing VOC_R (Fig. S3). Further, we investigated the influence of air mass aging on missing VOC_R. The ratio of ethylbenzene to m,p-xylene was used to characterize the degree of air mass aging (de Gouw et al., 2005; Yuan et al., 2013). A higher ratio of ethylbenzene to m,p-xylene corresponds to a higher degree of air mass aging as the m,p-xylene has a larger reaction rate constant (18.9×10^{-12} cm^3 $molecule^{-1}$ s^{-1}) than ethylbenzene (7.0×10^{-12} cm^3 $molecule^{-1}$ s^{-1}) when reacting with the major oxidant – OH radicals. As shown in Fig. 2e, missing VOC_R decreases with the ratio of ethylbenzene to m,p-xylene. Given that secondary production generally increased with air mass aging, this result further demonstrates that missing VOC_R was not caused by enhanced secondary production.

During the high missing-VOC_R days, the correlation coefficient for missing VOC_R versus CO is 0.76 (Fig. 3a), which is higher than that in the whole measurement period (0.56) shown in Fig. 2a. We then quantify the sources of missing VOC_R during the high missing-VOC_R days by applying MLR. The fitted coefficients are as follows: a is 0.031 s^{-1} ppb^{-1}, b is 0.012 s^{-1} ppb^{-1}, c is 1.8 s^{-1} ppb^{-1}, and $C_{background}$ is 1.3 s^{-1}. The coefficient of determination (R^2) for the MLR is 0.68. As shown in Fig. 3b, anthropogenic emissions were the largest contributor to missing VOC_R, accounting for 70 % of missing VOC_R. Secondary production, biogenic emissions, and background contribution played a minor role in missing VOC_R (13 %, 7 %, and 10 %, respectively). The parametric relationship between missing VOC_R and relevant tracers established by MLR provides a valid approach to estimate the missing VOC_R according to readily available gases, including CO, O_X, and isoprene.

Although anthropogenic emissions are identified as the major source of missing VOC_R, which species dominantly contributes to the missing VOC_R remains unclear. A potential source is the unmeasured branched alkenes because of their high reactivity previously observed from vehicle exhaust (Nakashima et al., 2010) and gasoline evaporation emissions (Wu et al., 2015). Another possible source is emitted OVOCs with a more complex functional group that cannot be accurately measured. In addition, directly emitted semivolatile and intermediate-volatility organic compounds are also possible sources of missing VOC_R (Stewart et al., 2021).

3.3 The impact of missing VOC_R on O_3 sensitivity regimes

The reaction of OH with VOCs is key to the propagation and amplification of OH radicals, thus determining the ozone production rate (Tonnesen and Dennis, 2000). The box model was used to evaluate the impact of missing VOC_R on the O_3 production rate during high missing-VOC_R days. The settings of model simulations for different scenarios are de-

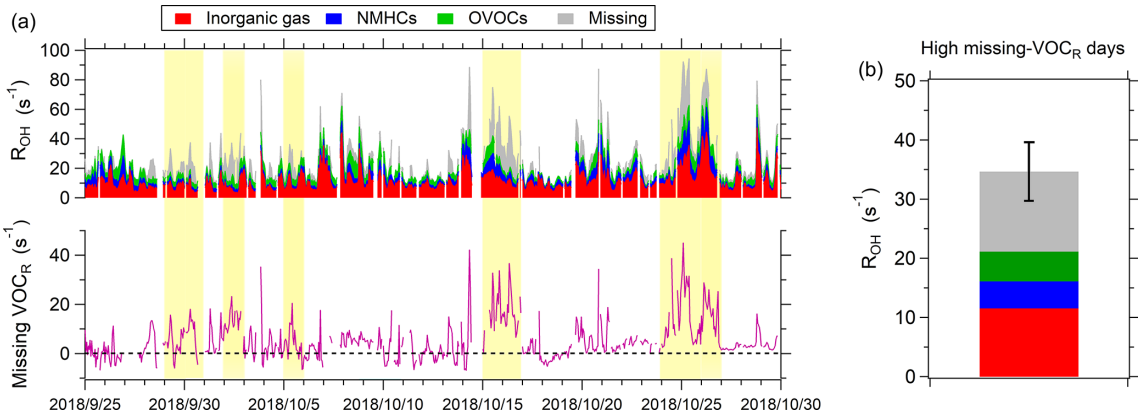

Figure 1. The level of missing VOC_R during the measurements in Guangzhou. **(a)** Time series of measured R_{OH} and calculated R_{OH} from all measured reactive gases in Guangzhou. Yellow background represents the high missing-VOC_R days, with missing VOC_R accounting for more than 30 % of the total R_{OH}. **(b)** Contributions of different compositions to R_{OH} on high missing-VOC_R days. The error bar represents the standard deviation of missing VOC_R.

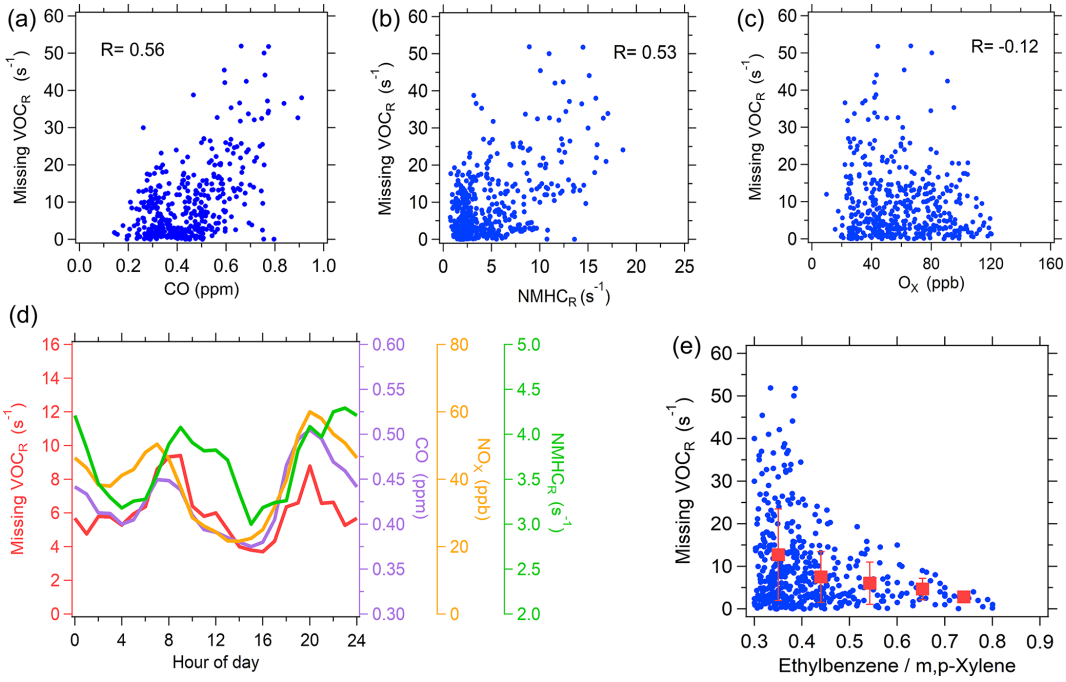

Figure 2. Correlation of missing VOC_R with major tracers during the whole measurement period. **(a–c)** Correlation of missing VOC_R with CO, OH reactivity of NMHCs ($NMHC_R$), and O_X. Each point represents hourly data. **(d)** Diurnal variations in missing VOC_R, CO, NO_X, and NMHCs. **(e)** The dependence of missing VOC_R on the ethylbenzene / m,p-xylene ratio. The red squares indicate the mean values of missing VOC_R in different ranges of the ratio of ethylbenzene to m,p-xylene with a classification width of 0.1, and the error bars represent the standard deviation.

picted in Sect. 2.6. In the base scenario, on average, the measured VOC_Rs of n-pentane, ethylene, toluene, and all 56 NMHCs are 0.14, 0.53, 0.60, and 4.6 s^{-1}, respectively. To consider the missing VOC_R (an average of 13 s^{-1}) in the model, four scenarios were simulated by additionally increasing n-pentane, ethylene, toluene, and 56 NMHCs by factors of 70, 16, 13.3, and 1.9, respectively. These increasing factors led to an additional increase in VOC_R of both NMHCs and unconstrained secondary products, which exactly compensated for the missing VOC_R. Figure 4 shows the simulated $P(O_3)$ for the base scenario and the scenarios considering missing VOC_R. The daytime average $P(O_3)$ in the scenarios considering missing VOC_R is a factor of 1.5–4.5 for the results in the base scenario. The difference in the added species has a large effect on $P(O_3)$. Adding toluene causes a larger increase in $P(O_3)$ than adding n-pentane or

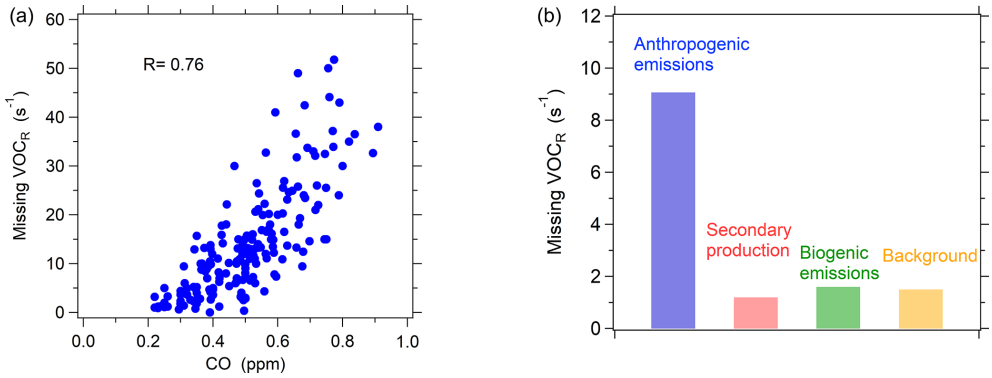

Figure 3. The source apportionment of missing VOC_R on high missing-VOC_R days. **(a)** Correlation of missing VOC_R with CO. Each point represents hourly data. **(b)** Contributions of different sources to missing VOC_R according to the MLR.

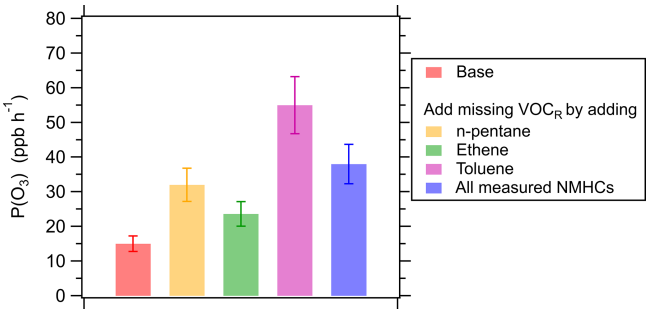

Figure 4. Simulated daytime mean $P(O_3)$ for the base scenario (without missing VOC_R) and the scenario considering missing VOC_R, respectively, on high missing-VOC_R days. The missing VOC_R is considered by adding individual species (n-pentane, ethene, or toluene) or increasing all measured NMHCs to compensate for the missing VOC_R. The error bar represents the standard deviation of $P(O_3)$ induced by the uncertainty of the missing VOC_R.

ethene, as toluene has a stronger ability to amplify the production of radicals.

O_3 precursor sensitivity depends on the dominant loss pathways of RO_X radicals ($RO_X = OH + HO_2 + RO_2$). O_3 production is NO_X-limited if the self-reaction of peroxy radicals (HO_2 and RO_2) dominates the RO_X sink and VOC-limited if the reaction of NO_2 with OH dominates (Kleinman et al., 1997, 2001). Accordingly, the ratio of the RO_X sink induced by $OH + NO_2$ reaction to the total rate of the two RO_X sinks, i.e., L_N/Q, is used to identify O_3 sensitivity regimes. O_3 production is NO_X-limited if L_N/Q is lower than 0.5; otherwise, it is VOC-limited (Kleinman et al., 1997).

$$L_N/Q = \frac{k_{OH+NO_2}[OH][NO_2]}{k_{HO_2+RO_2}[HO_2][RO_2] + k_{HO_2+HO_2}[HO_2][HO_2] + k_{OH+HO_2}[OH][HO_2] + k_{OH+NO_2}[OH][NO_2]} \quad (7)$$

As shown in Fig. 5a, in the base scenario, L_N/Q remained at a stable and high level (> 0.9) during the daytime, when photochemical production of ozone occurs, indicating that O_3 production was VOC-limited. In the scenarios considering missing VOC_R, L_N/Q decreased significantly regardless of which VOC species was added, compared to the base scenario. Adding toluene caused the largest decrease in L_N/Q, followed by adding all measured NMHC species, adding the alkane, and adding the alkene. It is worth noting that adding toluene and all measured NMHC species caused the L_N/Q to be close to 0.5 in the afternoon, indicating that the O_3 production shifted to transitional or NO_X-limited regimes in these scenarios. Figure 5b shows the changes in radical sinks before and after considering missing VOC_R. All radical sinks including self-reactions of peroxy radicals and $OH + NO_2$ reaction increased after considering missing VOC_R. Nevertheless, the increased proportion of the self-reactions of peroxy radicals was larger than that of $OH + NO_2$ reaction, leading to a decrease in L_N/Q and thus a shift toward an NO_X-limited regime.

Figure 5c shows the dependence of daily peak O_3 concentrations on NO_X concentrations, which was calculated by the box model for the base scenario and the scenario considering missing VOC_R. The NO_X concentration level corresponding to the maximum of O_3 concentrations was determined. This NO_X concentration level reflects the threshold for distinguishing between VOC-limited and NO_X-limited regimes. The larger threshold of NO_X represents a higher possibility of ozone production in an NO_X-limited regime. The threshold of NO_X for the scenario considering missing VOC_R is 46 % higher than for the base scenario. Note that the uncertainty in missing VOC_R leads to 17 % uncertainty in the threshold of NO_X for the scenario considering missing VOC_R. Overall, Fig. 5 suggests that omitting the missing VOC_R will overestimate the degree of the VOC-limited regime and thus overestimate the effect of VOC abatement in reducing ozone pollution, which in turn may mislead ozone control strategy.

3.4 Atmospheric implications

Although many previous studies have reported that photochemical production processes and biogenic emissions are

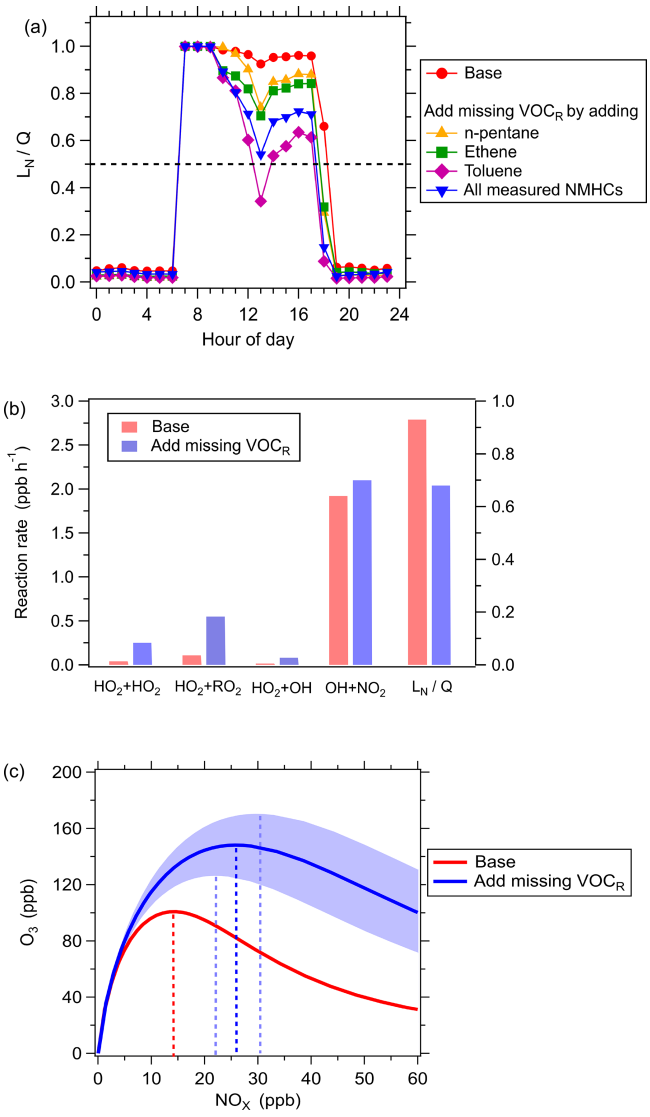

Figure 5. The impact of missing VOC_R on O_3 sensitivity for the high-missing VOC_R days. **(a)** Diurnal variations in L_N/Q for the base scenario and the scenarios considering missing VOC_R. The missing VOC_R is considered by adding individual species (*n*-pentane, ethene, or toluene) or increasing all measured NMHCs to fill the missing VOC_R. The dashed line represents the threshold value of L_N/Q that distinguishes VOC-limited and NO_X-limited regimes. **(b)** The averages of radical sinks in the afternoon (12:00–18:00) for the base scenario (red bar) and the scenario considering missing VOC_R (blue bar) by increasing all measured NMHCs to fill the missing VOC_R. **(c)** Model-simulated dependence of daily peak O_3 concentrations on daily mean NO_X concentrations for the base scenario (red curve) and the scenario considering missing VOC_R (blue curve) by increasing all measured NMHCs to fill the missing VOC_R. The dashed lines parallel to the *y* axis represent the threshold of NO_X levels for distinguishing between VOC-limited and NO_X-limited regimes. The shaded area represents the standard deviation induced by the uncertainty in the missing VOC_R.

important sources of missing VOC_R (Lou et al., 2010; Dolgorouky et al., 2012; Yang et al., 2017; Sanchez et al., 2021; Di Carlo et al., 2004), we find that anthropogenic emissions may dominate the missing VOC_R in urban regions. In zero-dimensional box models and three-dimensional chemistry-transport models, the input of VOC emission information mainly contains well-studied simple-structure alkanes, alkenes, and aromatics, while those unmeasured or unknown VOC species have been neglected. This will lead to biases in quantifying ozone production and diagnosing ozone sensitivity regimes. Our study demonstrates that the ambient measurement of R_{OH} at urban sites can provide quantification of missing VOC_R, which can be used in models to account for the missing VOC_R from anthropogenic emissions. In addition, the parametric equation of missing VOC_R derived from the MLR method (Eq. 4) can be used here to estimate missing VOC_R according to measurements of CO, O_X, and isoprene. Further study should try to parse the specific sources of the missing VOC_R, e.g., whether the missing VOC_R is from intermediate-volatility and semivolatile organic compounds emitted from vehicles or whether it is from some other sources. Furthermore, future studies can focus on direct measurements of missing VOC_R for various emission sources to develop a comprehensive emission inventory of missing VOC_R, which will help to improve O_3 pollution mitigation strategies.

Data availability. The observational data and the model code used in this study are available from the corresponding authors upon request (byuan@jnu.edu.cn).

Supplement. The supplement related to this article is available online at: https://doi.org/10.5194/acp-24-4017-2024-supplement.

Author contributions. BY and WW designed the research. WW and BY prepared the manuscript with contributions from the other authors. WW performed the data analysis with contributions from HS, YC, FB, CX, and CM. JQ, SW, WS, XW, HW, SL, and MS collected data.

Competing interests. At least one of the (co-)authors is a member of the editorial board of *Atmospheric Chemistry and Physics*. The peer-review process was guided by an independent editor, and the authors also have no other competing interests to declare.

Disclaimer. Publisher's note: Copernicus Publications remains neutral with regard to jurisdictional claims made in the text, published maps, institutional affiliations, or any other geographical representation in this paper. While Copernicus Publications makes every effort to include appropriate place names, the final responsibility lies with the authors.

Acknowledgements. This work was supported by the National Natural Science Foundation of China (grant nos. 42121004, 42275103, 42230701, and 42175135). This work was also supported by the Special Fund Project for Science and Technology Innovation Strategy of Guangdong Province (grant no. 2019B121205004).

Financial support. This research has been supported by the National Natural Science Foundation of China (grant nos. 42121004, 42275103, 42230701, and 42175135).

The article processing charges for this open-access publication were covered by the Max Planck Society.

Review statement. This paper was edited by Rob MacKenzie and reviewed by two anonymous referees.

References

Atkinson, R.: Atmospheric chemistry of VOCs and NO_x, Atmos. Environ., 34, 2063–2101, 2000.

Atkinson, R. and Arey, J.: Atmospheric degradation of volatile organic compounds, Chem. Rev., 103, 4605–4638, 2003.

Burkholder, J., Sander, S., Abbatt, J., Barker, J., Cappa, C., Crounse, J., Dibble, T., Huie, R., Kolb, C., and Kurylo, M.: Chemical kinetics and photochemical data for use in atmospheric studies, evaluation number 19, Pasadena, CA, JPL Publication 19-5, Jet Propulsion Laboratory, National Aeronautics and Space Administration, http://jpldataeval.jpl.nasa.gov (last access: 26 March 2024), 2020.

de Gouw, J. A., Warneke, C., Parrish, D. D., Holloway, J. S., Trainer, M., and Fehsenfeld, F. C.: Emission sources and ocean uptake of acetonitrile (CH_3CN) in the atmosphere, J. Geophys. Res.-Atmos., 108, 4329, https://doi.org/10.1029/2002JD002897, 2003.

de Gouw, J., Middlebrook, A., Warneke, C., Goldan, P., Kuster, W., Roberts, J., Fehsenfeld, F., Worsnop, D., Canagaratna, M., and Pszenny, A.: Budget of organic carbon in a polluted atmosphere: Results from the New England Air Quality Study in 2002, J. Geophys. Res.-Atmos., 110, D16305, https://doi.org/10.1029/2004JD005623, 2005.

Di Carlo, P., Brune, W. H., Martinez, M., Harder, H., Lesher, R., Ren, X. R., Thornberry, T., Carroll, M. A., Young, V., Shepson, P. B., Riemer, D., Apel, E., and Campbell, C.: Missing OH reactivity in a forest: Evidence for unknown reactive biogenic VOCs, Science, 304, 722–725, https://doi.org/10.1126/science.1094392, 2004.

Dolgorouky, C., Gros, V., Sarda-Esteve, R., Sinha, V., Williams, J., Marchand, N., Sauvage, S., Poulain, L., Sciare, J., and Bonsang, B.: Total OH reactivity measurements in Paris during the 2010 MEGAPOLI winter campaign, Atmos. Chem. Phys., 12, 9593–9612, https://doi.org/10.5194/acp-12-9593-2012, 2012.

Fuchs, H., Tan, Z., Lu, K., Bohn, B., Broch, S., Brown, S. S., Dong, H., Gomm, S., Häseler, R., He, L., Hofzumahaus, A., Holland, F., Li, X., Liu, Y., Lu, S., Min, K. E., Rohrer, F., Shao, M., Wang, B., Wang, M., Wu, Y., Zeng, L., Zhang, Y., Wahner, A., and Zhang, Y.: OH reactivity at a rural site (Wangdu) in the North China Plain: contributions from OH reactants and experimental OH budget, Atmos. Chem. Phys., 17, 645–661, https://doi.org/10.5194/acp-17-645-2017, 2017.

Goldstein, A. H. and Galbally, I. E.: Known and unexplored organic constituents in the earth's atmosphere, Environ. Sci. Technol., 41, 1514–1521, 2007.

Griffith, S. M., Hansen, R., Dusanter, S., Michoud, V., Gilman, J., Kuster, W., Veres, P., Graus, M., de Gouw, J., and Roberts, J.: Measurements of hydroxyl and hydroperoxy radicals during CalNex-LA: Model comparisons and radical budgets, J. Geophys. Res.-Atmos., 121, 4211–4232, 2016.

Hansen, R. F., Griffith, S. M., Dusanter, S., Rickly, P. S., Stevens, P. S., Bertman, S. B., Carroll, M. A., Erickson, M. H., Flynn, J. H., Grossberg, N., Jobson, B. T., Lefer, B. L., and Wallace, H. W.: Measurements of total hydroxyl radical reactivity during CABINEX 2009 – Part 1: field measurements, Atmos. Chem. Phys., 14, 2923–2937, https://doi.org/10.5194/acp-14-2923-2014, 2014.

Hansen, R. F., Blocquet, M., Schoemaecker, C., Léonardis, T., Locoge, N., Fittschen, C., Hanoune, B., Stevens, P. S., Sinha, V., and Dusanter, S.: Intercomparison of the comparative reactivity method (CRM) and pump–probe technique for measuring total OH reactivity in an urban environment, Atmos. Meas. Tech., 8, 4243–4264, https://doi.org/10.5194/amt-8-4243-2015, 2015.

Jenkin, M. E., Saunders, S. M., Wagner, V., and Pilling, M. J.: Protocol for the development of the Master Chemical Mechanism, MCM v3 (Part B): tropospheric degradation of aromatic volatile organic compounds, Atmos. Chem. Phys., 3, 181–193, https://doi.org/10.5194/acp-3-181-2003, 2003.

Kleinman, L. I.: Low and high NO_x tropospheric photochemistry, J. Geophys. Res.-Atmos., 99, 16831–16838, 1994.

Kleinman, L. I., Daum, P. H., Lee, J. H., Lee, Y. N., Nunnermacker, L. J., Springston, S. R., Newman, L., Weinstein-Lloyd, J., and Sillman, S.: Dependence of ozone production on NO and hydrocarbons in the troposphere, Geophys. Res. Lett., 24, 2299–2302, 1997.

Kleinman, L. I., Daum, P. H., Lee, Y. N., Nunnermacker, L. J., Springston, S. R., Weinstein-Lloyd, J., and Rudolph, J.: Sensitivity of ozone production rate to ozone precursors, Geophys. Res. Lett., 28, 2903–2906, 2001.

Kovacs, T., Brune, W., Harder, H., Martinez, M., Simpas, J., Frost, G., Williams, E., Jobson, T., Stroud, C., and Young, V.: Direct measurements of urban OH reactivity during Nashville SOS in summer 1999, J. Environ. Monitor., 5, 68–74, 2003.

Lefohn, A. S., Malley, C. S., Smith, L., Wells, B., Hazucha, M., Simon, H., Naik, V., Mills, G., Schultz, M. G., and Paoletti, E.: Tropospheric ozone assessment report: Global ozone metrics for climate change, human health, and crop/ecosystem research, Elem. Sci. Anth., 6, 27, https://doi.org/10.1525/elementa.279, 2018.

Li, K., Jacob, D. J., Liao, H., Shen, L., Zhang, Q., and Bates, K. H.: Anthropogenic drivers of 2013–2017 trends in summer surface ozone in China, P. Natl. Acad. Sci. USA, 116, 422–427, 2019.

Li, X.-B., Yuan, B., Parrish, D. D., Chen, D., Song, Y., Yang, S., Liu, Z., and Shao, M.: Long-term trend of ozone in southern China reveals future mitigation strategy for air pollution, Atmos. Environ., 269, 118869, https://doi.org/10.1016/j.atmosenv.2021.118869, 2022.

Lou, S., Holland, F., Rohrer, F., Lu, K., Bohn, B., Brauers, T., Chang, C. C., Fuchs, H., Häseler, R., Kita, K., Kondo, Y., Li, X., Shao, M., Zeng, L., Wahner, A., Zhang, Y., Wang, W., and Hofzumahaus, A.: Atmospheric OH reactivities in the Pearl River Delta – China in summer 2006: measurement and model results, Atmos. Chem. Phys., 10, 11243–11260, https://doi.org/10.5194/acp-10-11243-2010, 2010.

Lu, K. D., Hofzumahaus, A., Holland, F., Bohn, B., Brauers, T., Fuchs, H., Hu, M., Häseler, R., Kita, K., Kondo, Y., Li, X., Lou, S. R., Oebel, A., Shao, M., Zeng, L. M., Wahner, A., Zhu, T., Zhang, Y. H., and Rohrer, F.: Missing OH source in a suburban environment near Beijing: observed and modelled OH and HO2 concentrations in summer 2006, Atmos. Chem. Phys., 13, 1057–1080, https://doi.org/10.5194/acp-13-1057-2013, 2013.

Lu, X., Hong, J. Y., Zhang, L., Cooper, O. R., Schultz, M. G., Xu, X. B., Wang, T., Gao, M., Zhao, Y. H., and Zhang, Y. H.: Severe Surface Ozone Pollution in China: A Global Perspective, Environ. Sci. Technol. Lett., 5, 487–494, https://doi.org/10.1021/acs.estlett.8b00366, 2018.

Mihelcic, D., Holland, F., Hofzumahaus, A., Hoppe, L., Konrad, S., Müsgen, P., Pätz, H. W., Schäfer, H. J., Schmitz, T., and Volz-Thomas, A.: Peroxy radicals during BERLIOZ at Pabstthum: Measurements, radical budgets and ozone production, J. Geophys. Res.-Atmos., 108, 8254, https://doi.org/10.1029/2001JD001014, 2003.

Monks, P. S., Archibald, A. T., Colette, A., Cooper, O., Coyle, M., Derwent, R., Fowler, D., Granier, C., Law, K. S., Mills, G. E., Stevenson, D. S., Tarasova, O., Thouret, V., von Schneidemesser, E., Sommariva, R., Wild, O., and Williams, M. L.: Tropospheric ozone and its precursors from the urban to the global scale from air quality to short-lived climate forcer, Atmos. Chem. Phys., 15, 8889–8973, https://doi.org/10.5194/acp-15-8889-2015, 2015.

Nakashima, Y., Kamei, N., Kobayashi, S., and Kajii, Y.: Total OH reactivity and VOC analyses for gasoline vehicular exhaust with a chassis dynamometer, Atmos. Environ., 44, 468–475, https://doi.org/10.1016/j.atmosenv.2009.11.006, 2010.

Nakashima, Y., Kato, S., Greenberg, J., Harley, P., Karl, T., Turnipseed, A., Apel, E., Guenther, A., Smith, J., and Kajii, Y.: Total OH reactivity measurements in ambient air in a southern Rocky mountain ponderosa pine forest during BEACHON-SRM08 summer campaign, Atmos. Environ., 85, 1–8, https://doi.org/10.1016/j.atmosenv.2013.11.042, 2014.

Nölscher, A. C., Yañez-Serrano, A. M., Wolff, S., de Araujo, A. C., Lavrič, J. V., Kesselmeier, J., and Williams, J.: Unexpected seasonality in quantity and composition of Amazon rainforest air reactivity, Nat. Commun., 7, 10383, https://doi.org/10.1038/ncomms10383, 2016.

Paoletti, E., De Marco, A., Beddows, D. C., Harrison, R. M., and Manning, W. J.: Ozone levels in European and USA cities are increasing more than at rural sites, while peak values are decreasing, Environ. Pollut., 192, 295–299, 2014.

Praplan, A. P., Tykka, T., Chen, D., Boy, M., Taipale, D., Vakkari, V., Zhou, P. T., Petaja, T., and Hellen, H.: Long-term total OH reactivity measurements in a boreal forest, Atmos. Chem. Phys., 19, 14431–14453, https://doi.org/10.5194/acp-19-14431-2019, 2019.

Sadanaga, Y., Yoshino, A., Kato, S., and Kajii, Y.: Measurements of OH reactivity and photochemical ozone production in the urban atmosphere, Environ. Sci. Technol., 39, 8847–8852, 2005.

Sanchez, D., Seco, R., Gu, D., Guenther, A., Mak, J., Lee, Y., Kim, D., Ahn, J., Blake, D., Herndon, S., Jeong, D., Sullivan, J. T., McGee, T., Park, R., and Kim, S.: Contributions to OH reactivity from unexplored volatile organic compounds measured by PTR-ToF-MS – a case study in a suburban forest of the Seoul metropolitan area during the Korea–United States Air Quality Study (KORUS-AQ) 2016, Atmos. Chem. Phys., 21, 6331–6345, https://doi.org/10.5194/acp-21-6331-2021, 2021.

Sekimoto, K., Li, S.-M., Yuan, B., Koss, A., Coggon, M., Warneke, C., and de Gouw, J.: Calculation of the sensitivity of proton-transfer-reaction mass spectrometry (PTR-MS) for organic trace gases using molecular properties, Int. J. Mass Spectrom., 421, 71–94, https://doi.org/10.1016/j.ijms.2017.04.006, 2017.

Shetter, R. E. and Müller, M.: Photolysis frequency measurements using actinic flux spectroradiometry during the PEM-Tropics mission: Instrumentation description and some results, J. Geophys. Res.-Atmos., 104, 5647–5661, https://doi.org/10.1029/98JD01381, 1999.

Shirley, T. R., Brune, W. H., Ren, X., Mao, J., Lesher, R., Cardenas, B., Volkamer, R., Molina, L. T., Molina, M. J., Lamb, B., Velasco, E., Jobson, T., and Alexander, M.: Atmospheric oxidation in the Mexico City Metropolitan Area (MCMA) during April 2003, Atmos. Chem. Phys., 6, 2753–2765, https://doi.org/10.5194/acp-6-2753-2006, 2006.

Sillman, S., Logan, J. A., and Wofsy, S. C.: The sensitivity of ozone to nitrogen oxides and hydrocarbons in regional ozone episodes, J. Geophys. Res.-Atmos., 95, 1837–1851, 1990.

Sinha, V., Williams, J., Crowley, J. N., and Lelieveld, J.: The Comparative Reactivity Method – a new tool to measure total OH Reactivity in ambient air, Atmos. Chem. Phys., 8, 2213–2227, https://doi.org/10.5194/acp-8-2213-2008, 2008.

Song, K., Gong, Y., Guo, S., Lv, D., Wang, H., Wan, Z., Yu, Y., Tang, R., Li, T., Tan, R., Zhu, W., Shen, R., and Lu, S.: Investigation of partition coefficients and fingerprints of atmospheric gas- and particle-phase intermediate volatility and semi-volatile organic compounds using pixel-based approaches, J. Chromatogr. A, 1665, 462808, https://doi.org/10.1016/j.chroma.2022.462808, 2022.

Stewart, G. J., Nelson, B. S., Acton, W. J. F., Vaughan, A. R., Farren, N. J., Hopkins, J. R., Ward, M. W., Swift, S. J., Arya, R., Mondal, A., Jangirh, R., Ahlawat, S., Yadav, L., Sharma, S. K., Yunus, S. S. M., Hewitt, C. N., Nemitz, E., Mullinger, N., Gadi, R., Sahu, L. K., Tripathi, N., Rickard, A. R., Lee, J. D., Mandal, T. K., and Hamilton, J. F.: Emissions of intermediate-volatility and semi-volatile organic compounds from domestic fuels used in Delhi, India, Atmos. Chem. Phys., 21, 2407–2426, https://doi.org/10.5194/acp-21-2407-2021, 2021.

Tonnesen, G. S. and Dennis, R. L.: Analysis of radical propagation efficiency to assess ozone sensitivity to hydrocarbons and NO_x: 1. Local indicators of instantaneous odd oxygen production sensitivity, J. Geophys. Res.-Atmos., 105, 9213–9225, 2000.

Wang, C., Yuan, B., Wu, C., Wang, S., Qi, J., Wang, B., Wang, Z., Hu, W., Chen, W., Ye, C., Wang, W., Sun, Y., Wang, C., Huang, S., Song, W., Wang, X., Yang, S., Zhang, S., Xu, W., Ma, N., Zhang, Z., Jiang, B., Su, H., Cheng, Y., Wang, X., and Shao, M.: Measurements of higher alkanes using NO^+ chemical ionization in PTR-ToF-MS: important contributions of higher alkanes to secondary organic aerosols in China, Atmos. Chem.

Phys., 20, 14123–14138, https://doi.org/10.5194/acp-20-14123-2020, 2020.

Wang, H., Zhang, X., and Chen, Z.: Development of DNPH/H-PLC method for the measurement of carbonyl compounds in the aqueous phase: applications to laboratory simulation and field measurement, Environ. Chem., 6, 389–397, https://doi.org/10.1071/EN09057, 2009.

Wang, M., Zeng, L., Lu, S., Shao, M., Liu, X., Yu, X., Chen, W., Yuan, B., Zhang, Q., and Hu, M.: Development and validation of a cryogen-free automatic gas chromatograph system (GC-MS/FID) for online measurements of volatile organic compounds, Anal. Method., 6, 9424–9434, 2014.

Wang, Q. Q., Shao, M., Liu, Y., William, K., Paul, G., Li, X. H., Liu, Y. A., and Lu, S. H.: Impact of biomass burning on urban air quality estimated by organic tracers: Guangzhou and Beijing as cases, Atmos. Environ., 41, 8380–8390, https://doi.org/10.1016/j.atmosenv.2007.06.048, 2007.

Wang, W., Li, X., Shao, M., Hu, M., Zeng, L., Wu, Y., and Tan, T.: The impact of aerosols on photolysis frequencies and ozone production in Beijing during the 4-year period 2012–2015, Atmos. Chem. Phys., 19, 9413–9429, https://doi.org/10.5194/acp-19-9413-2019, 2019.

Wang, W., Parrish, D. D., Li, X., Shao, M., Liu, Y., Mo, Z., Lu, S., Hu, M., Fang, X., Wu, Y., Zeng, L., and Zhang, Y.: Exploring the drivers of the increased ozone production in Beijing in summertime during 2005–2016, Atmos. Chem. Phys., 20, 15617–15633, https://doi.org/10.5194/acp-20-15617-2020, 2020.

Wang, W., Parrish, D. D., Wang, S., Bao, F., Ni, R., Li, X., Yang, S., Wang, H., Cheng, Y., and Su, H.: Long-term trend of ozone pollution in China during 2014–2020: distinct seasonal and spatial characteristics and ozone sensitivity, Atmos. Chem. Phys., 22, 8935–8949, https://doi.org/10.5194/acp-22-8935-2022, 2022.

Wu, C., Wang, C., Wang, S., Wang, W., Yuan, B., Qi, J., Wang, B., Wang, H., Wang, C., Song, W., Wang, X., Hu, W., Lou, S., Ye, C., Peng, Y., Wang, Z., Huangfu, Y., Xie, Y., Zhu, M., Zheng, J., Wang, X., Jiang, B., Zhang, Z., and Shao, M.: Measurement report: Important contributions of oxygenated compounds to emissions and chemistry of volatile organic compounds in urban air, Atmos. Chem. Phys., 20, 14769–14785, https://doi.org/10.5194/acp-20-14769-2020, 2020.

Wu, Y., Yang, Y. D., Shao, M., and Lu, S. H.: Missing in total OH reactivity of VOCs from gasoline evaporation, Chinese Chem. Lett., 26, 1246–1248, https://doi.org/10.1016/j.cclet.2015.05.047, 2015.

Xie, X., Shao, M., Liu, Y., Lu, S., Chang, C.-C., and Chen, Z.-M.: Estimate of initial isoprene contribution to ozone formation potential in Beijing, China, Atmos. Environ., 42, 6000–6010, 2008.

Xu, R., Li, X., Dong, H., Lv, D., Kim, N., Yang, S., Wang, W., Chen, J., Shao, M., and Lu, S.: Field observations and quantifications of atmospheric formaldehyde partitioning in gaseous and particulate phases, Sci. Total Environ., 808, 152122, https://doi.org/10.1016/j.scitotenv.2021.152122, 2022.

Yang, Y., Liao, H., and Lou, S.: Increase in winter haze over eastern China in recent decades: Roles of variations in meteorological parameters and anthropogenic emissions, J. Geophys. Res.-Atmos., 121, 13050–13065, https://doi.org/10.1002/2016JD025136, 2016a.

Yang, Y., Shao, M., Wang, X., Nölscher, A. C., Kessel, S., Guenther, A., and Williams, J.: Towards a quantitative understanding of total OH reactivity: A review, Atmos. Environ., 134, 147–161, 2016b.

Yang, Y., Shao, M., Keßel, S., Li, Y., Lu, K., Lu, S., Williams, J., Zhang, Y., Zeng, L., Nölscher, A. C., Wu, Y., Wang, X., and Zheng, J.: How the OH reactivity affects the ozone production efficiency: case studies in Beijing and Heshan, China, Atmos. Chem. Phys., 17, 7127–7142, https://doi.org/10.5194/acp-17-7127-2017, 2017.

Yoshino, A., Sadanaga, Y., Watanabe, K., Kato, S., Miyakawa, Y., Matsumoto, J., and Kajii, Y.: Measurement of total OH reactivity by laser-induced pump and probe technique – comprehensive observations in the urban atmosphere of Tokyo, Atmos. Environ., 40, 7869–7881, https://doi.org/10.1016/j.atmosenv.2006.07.023, 2006.

Yu, Y., Cheng, P., Li, H., Yang, W., Han, B., Song, W., Hu, W., Wang, X., Yuan, B., Shao, M., Huang, Z., Li, Z., Zheng, J., Wang, H., and Yu, X.: Budget of nitrous acid (HONO) at an urban site in the fall season of Guangzhou, China, Atmos. Chem. Phys., 22, 8951–8971, https://doi.org/10.5194/acp-22-8951-2022, 2022.

Yuan, B., Chen, W., Shao, M., Wang, M., Lu, S., Wang, B., Liu, Y., Chang, C.-C., and Wang, B.: Measurements of ambient hydrocarbons and carbonyls in the Pearl River Delta (PRD), China, Atmos. Res., 116, 93–104, 2012.

Yuan, B., Hu, W. W., Shao, M., Wang, M., Chen, W. T., Lu, S. H., Zeng, L. M., and Hu, M.: VOC emissions, evolutions and contributions to SOA formation at a receptor site in eastern China, Atmos. Chem. Phys., 13, 8815–8832, https://doi.org/10.5194/acp-13-8815-2013, 2013.

Yuan, B., Koss, A. R., Warneke, C., Coggon, M., Sekimoto, K., and de Gouw, J. A.: Proton-Transfer-Reaction Mass Spectrometry: Applications in Atmospheric Sciences, Chem. Rev., 117, 13187–13229, https://doi.org/10.1021/acs.chemrev.7b00325, 2017.